J Assist Reprod Genet (2017) 34:535–545
DOI 10.1007/s10815-017-0872-z

REPRODUCTIVE PHYSIOLOGY AND DISEASE

# Long-term effects of repeated superovulation on the uterus and mammary gland in rhesus monkeys

**Peipei Yan[1] · Jingyi Xu[1] · Yan Zeng[1] · Guoying Dong[1] · Huarong Cao[1] · Meimei Zheng[1] · Hui Zhu[1]**

Received: 8 October 2016 / Accepted: 9 January 2017 / Published online: 23 January 2017


**Abstract**
*Purpose* The aim of this study is to evaluate the effect of repeated controlled ovarian hyperstimulation (COH) on the structure and function of the uterus and mammary gland.
*Methods* Three adult female rhesus monkeys were superovulated up to four times, and three spontaneously ovulating monkeys were used as controls. After a 5-year period, the uterus and mammary gland tissue samples were collected for examination of their structure and function. Further, the expression of certain tumor markers was examined to assess the cancer risk for each organ.
*Results* Expression of Wnt7a (associated with the functional/developmental status of the uterus) was significantly decreased in the uterus of superovulated monkeys, and decreased expression of proliferation marker PCNA was found in uterine cells. Meanwhile, abnormal Golgi-derived secretory vesicles with an irregular shape were observed in the mammary glands of the superovulated monkeys, and decreased PCNA expression together with increased expression of caspase-3 (an apoptosis marker) was indicated in the mammary cells. The expression of tumor molecular markers of the uterus and mammary gland was not significantly different between the two groups.
*Conclusions* Repeated COH affects the expression of the uterine development-related gene several years later, and uterine cells exhibited a low proliferation status. The ultrastructure of the mammary gland epithelial cells was abnormal, and the cells exhibited both low proliferation and high apoptosis status. Cancer risk for these organs was not observed. Given that primates are the closest relatives of humans, the results obtained from this study provide more intuitive information for optimization of clinical COH.

**Keywords** Safety assessment of ART · Controlled ovarian hyperstimulation (COH) · Uterus · Mammary gland · Rhesus monkey

## Introduction

Assisted reproductive technology (ART) is widely used to treat human infertility in the clinic. Controlled ovarian hyperstimulation (COH) is used routinely to obtain a higher number of fully mature fertilization-competent oocytes [1]. Because stimulated ovulation requires exogenous administration of gonadotropins [2], it is possible that non-physiological doses of the hormone will have adverse effects on maternal health, especially because most patients require more than one treatment cycle to achieve pregnancy [3]. Therefore, the influence of repeated COH on maternal health is an important topic that needs to be investigated.

In recent years, the adverse effects of repetitive induction of ovulation have caused profound concern, especially with regard to its effect on the ovary. Clinical studies have found that consecutive ovulation induction cycles can impair ovarian response and/or alter the quality of oocytes [4], but it is difficult to further study the exact aspects of ovarian and oocyte damage using the population sample. Therefore, animal models are gradually used for studying the potential effects of ARTs. Currently,

✉ Hui Zhu
njzhuhui@njmu.edu.cn

[1] State Key Laboratory of Reproductive Medicine, Department of Histology and Embryology, Nanjing Medical University, Nanjing 211166, China

animal studies are performed mainly using mice models; results indicate that repeated COH can induce oxidative damage and mitochondrial DNA mutations, alter the distribution of cytoplasmic organelles, and increase the incidence of spindle defects in the oocytes [5–7].

Although murine model studies have generated many interesting data, the differences between mice and humans cannot be ignored. Primates are closest to humans genetically; therefore, they are the preferred animal model, as they more accurately reflect the human physiological makeup. Such research outcomes using primates have more significance for clinical practice [8]. However, relatively few ART-related studies have been reported using primate models; only a few studies have employed the monkey model to assess the optimal dose of drugs that can induce ovulation in order to precipitate satisfactory ovarian responses [9, 10]. Recently, we used rhesus monkeys as a study model and demonstrated the long-term effect of repeated superovulation on the ovaries; this was evidenced by a change in the expression of a series of ovarian proteins that potentially affect the development and function of ovarian cells [11].

In addition to the potential effect on ovary structure and function, repeated ovulation induction has also been reportedly linked with an increased cancer risk of the female reproductive organs. A series of studies have indicated the potential association between repeated ovulation induction and the subsequent development of ovarian, uterine, mammary cancer, and the cancer risk augments with an increase in the time that has elapsed after COH [12–15]. However, there is no consensus on the cancer risk of repeated ovulation stimulation because some researchers have not observed an elevated risk in the treatment group [16, 17]. This may be due to numerous shortcomings of population studies, such as the wide differences in human populations, inconsistent drug exposure, and relatively short follow-up periods [18, 19]. Thus, it is necessary to determine the carcinogenic risk of repeated COH using animal models.

In view of the adverse effects on ovaries that have been confirmed by clinical and animal studies, we speculated that repeated ovulation induction may have adverse effects on two other female reproductive organs, the uterus and mammary glands. In this study, we will assess the potential influence of repeated COH on the uterus and mammary gland, using the non-human primate rhesus monkey as the study model. In view of our previous findings that repeated ovulation has long-term effects on the ovary, as well as the time-dependent risk of carcinogenesis, we evaluated the structure and function of the uterus and mammary gland at 5 years after repeat COH treatments.

## Materials and Methods

### Animals

We used six adult female rhesus monkeys (average age: 13 years) provided by the Kunming Primate Research Center (KPRC), People's Republic of China. The monkeys were individually caged and fed compound feed twice daily with ad libitum water in a controlled environment, and a photoperiod of 12 h light/12 h dark. Temperature was maintained between 20 and 24 °C, and humidity ranged between 40 and 60%. The six rhesus monkeys were divided into two groups: three of the rhesus monkeys underwent four cycles of ovarian stimulation (superovulation group) and the other three monkeys did not undergo any treatment (normal control group). We performed ovulation stimulation according to previously published experimental procedures [20].

### Tissue collection

Five years after repeated superovulation, the uterus tissue and mammary gland tissue samples were obtained at approximately day 10 of the menstrual cycle, which is the later period of endometrial proliferative phase. The uterus and mammary gland samples were divided into three parts: the first part was frozen in liquid nitrogen for protein and RNA extraction, the second part was fixed in 10% formaldehyde for histological examination, and the third part was maintained in 2.5% glutaraldehyde solution for ultrastructural examination.

### Histological and ultrastructural examination

The formaldehyde-fixed uterus and mammary gland tissues were embedded in paraffin. The samples were processed, sectioned into 5-μm-thick slices, and stained with hematoxylin and eosin for histologic examination. For ultrastructural examinations, tissue blocks of the mammary gland and uterus were postfixed in 2% $OsO_4$ and embedded in Araldite. Ultrathin sections were stained with uranyl acetate and lead citrate [11].

### Immunohistochemistry analysis

For the immunohistochemical analyses, the following primary antibodies were used: rabbit anti-estrogen receptor alpha (ERα) (1:50, Beijing ZhongShan Biotechnology Co., Beijing, China), rabbit anti-progesterone receptor (PR) (1:100, Beijing ZhongShan Biotechnology Co., Beijing, China), rabbit anti-$P16^{INK4a}$ (1:400, Proteintech, Chicago, USA), rabbit anti-Ki67 (1:200, Abcam, Cambridge, UK), and rabbit anti-phosphatase and tensin homolog (PTEN) (1:100, Boster, Wuhan, China). We performed immunohistochemical examination of the sections as follow. Briefly, the sections were incubated in 3%

hydrogen peroxide and washed in phosphate-buffered saline. We blocked nonspecific protein binding with bovine serum albumin. Sections were then incubated overnight at 4 °C with primary antibodies. Negative controls were incubated with rabbit IgG. After three washes in phosphate-buffered saline, the sections were incubated with horseradish peroxidase-conjugated secondary antibody. The DAB detection kit (Beijing ZhongShan Biotechnology Co. Beijing, China) was used for detecting the antibodies. The proportion of positive cells in five random high-power fields (×400) was determined, according to the specific compartment [21].

### TUNEL assay

The apoptotic analysis was performed both in the mammary gland tissue and the uterus tissue, using the terminal deoxyribonucleotidyl transferase (TdT)-mediated dUTP nick end-labeling method with an ApopTag Plus Peroxidase In Situ Apoptosis Detection Kit (Merck Millipore, Darmstadt, Germany), according to the manufacturer's instructions. The number of TUNEL-positive glandular epithelial cells with their nuclei stained brown was determined by counting the number of apoptotic cells in five randomly selected fields per animal under a ×400 magnification. The apoptosis index was calculated as the number of positive cells divided by the total number of cells.

### Real-time quantitative polymerase chain reaction

Total RNA was extracted from the uterus and mammary gland with the RNAprep pure tissue kit (TIANGEN, Beijing, China), according to the manufacturer's protocol. A 20-μl cDNA reaction volume was prepared using the PrimeScript RT reagent kit (TaKaRa, Dalian, China). SYBR Green Master Mix (High Rox Premixed) (Vazyme, Nanjing, China) was used for real-time polymerase chain reaction (PCR). The mRNA levels of nine uterus development/function-related genes (ERα, PR, wingless-type MMTV integration site family member 4 (Wnt4), Wnt5a, Wnt7a, β-catenin, homeobox (HOXA9, HOXA10, and HOXA11), two mammary gland development-related genes (ERα and PR), and four mammary gland tumor makers (ERα, PR, G-protein coupled estrogen receptor 1 (GPER1), and human epidermal receptor protein-2 (HER2)) were analyzed. Beta-actin was used as internal controls. The PCR thermal cycling parameters were as follows: 95 °C for 5 min, followed by 40 cycles of 95 °C for 10 s and 60 °C for 30 s. After PCR, a dissociation curve was constructed at 95 °C for 15 s, 60 °C for 60 s, and 95 °C for 15 s. The primer sequences and target fragment sizes are listed in Table 1.

**Table 1** Primer sequences and target fragment size of each gene

| Gene name | Sequence (5′ to 3′) | Amplicon size (bp) |
|---|---|---|
| ERα | AATCTGCCAAGGAGACTCGC<br>GGTTGGTGGCTGGACACATA | 147 |
| PR | GGCAATGGAAGGGCAGCATA<br>CATTTGGAATGCCCACTGGC | 215 |
| HER2 | CTGGAGTCCATTCTCCGACG<br>ATCAATGGTGCAGATGGGGG | 180 |
| GPER1 | CTCAGGCATTCGGCAGGTC<br>CTCACTCTCTGGGTACCTGG GTT | 135 |
| WNT4 | CCCTCATGAACCTCCACAAC<br>ACCTCACAGGAGCCTGACAC | 100 |
| WNT5a | CCAGGAGTTGCTTTGGGGAT<br>CATACCTAGCGACCACCAAGA | 126 |
| WNT7a | CCGAAAGATCCTGGAGGAGAA<br>TGAACGGCCTCGTTGTACTT | 147 |
| HOXA9 | CCCATCGATCCCAATAACCCA<br>ACCAGATCTTGACCTGCCTC | 193 |
| HOXA10 | GACTCCCTGGGCAATTCCAAA<br>CTAATCTCTAGGCGCCGCTC | 161 |
| HOXA11 | AAAGAGAAGCGCCTGCAACT<br>GGTCAGTGGATTCGCTGAGTA | 134 |
| β-catenin | GCTTGGAATGAGACTGCGGA<br>GATCTGGCAGCCCATCAACT | 202 |
| β-actin | TGACCCAGATCATGTTTGAG ACC<br>ATAGATGGGCACAGTGTGGG | 142 |

### Western blot analysis

Western blotting of mammary gland and uterus tissue lysates was performed as previously described [22]. In brief, protein from tissue lysates was separated on 10% polyacrylamide gels and transferred to PVDF membranes. The membranes were incubated for 2 h in 5% nonfat milk at room temperature and incubated overnight at 4 °C with primary rabbit anti-ERα (1:200), rabbit anti-PR (1:400), rabbit anti-$P16^{INK4a}$ (1:400), rabbit anti-Wnt7a (1:1000, abcam, Cambridge, UK), rabbit anti-HOXA10 (1:1000, Proteintech, Chicago, USA), rabbit anti-caspase3 (1:1000, Proteintech, Chicago, USA), mouse anti-proliferating cell nuclear antigen (PCNA) (1:500, Abbkine, CA, USA), rabbit anti-PTEN (1:100), and mouse anti-β-actin antibody (1:10,000, Merck Millipore, Darmstadt, Germany). After being washed three times in TBS, the membranes were incubated for 2 h with HRP-conjugated goat anti-rabbit IgG(H+L) (1:3000, Thermo Fisher Scientific Inc., Rockford, USA), or goat anti-mouse IgG(H+L) (Thermo Fisher Scientific Inc., Rockford, USA) at room temperature and washed again. The protein expression level was detected using an ECL kit and AlphaImager (GE Healthcare Bio-Sciences Corp., Piscataway, NJ).

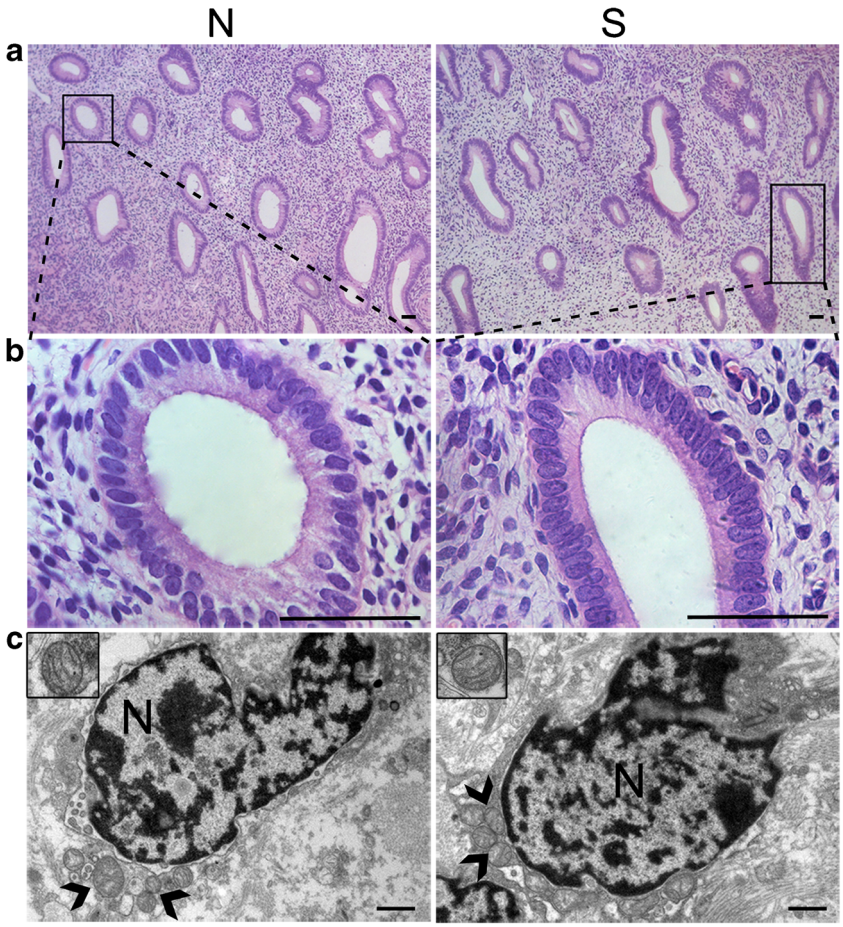


**Fig. 1** Structural analysis of the uterus: **a–b** Hematoxylin and eosin (HE) staining revealed that the uterus was normal in structure, with no discernible abnormalities in the morphological or histological characteristics of the uterine cells. Scale bar: 50 μm. **c** Normal ultrastructure of stromal cells was observed in the normal group and superovulation group (nuclei: *N*; mitochondria: ❯). Scale bar: 1 μm. *S* = superovulation group; *N* = normal group

### Statistical analysis

Data were expressed as mean ± standard deviation (SD). Statistical significance was determined using the unpaired two-tailed Student's *t* test. The results were considered statistically significant at $P < 0.05$.

## Results

### Structural assessment of the uterus and mammary gland

*Microscopic and ultramicroscopic structure of the uterus*

The wall of the uterus consists of three layers: perimetrium, myometrium, and endometrium. The endometrium is most relevant to the uterine function. The endometrium is composed of a simple columnar epithelial cell layer and the lamina propria. The uterine gland, stromal cells, and a large amount of connective tissue fibers are contained in the lamina propria. On observation of the endometrium, we found that the luminal epithelial cells were present in a single layer (which is their normal morphology) both in the superovulation group and in the normal group. No differences were found in the structure or number of the uterus gland between the two groups, and the histological structure of the glandular epithelial cells also showed no discernible abnormalities. Additionally, the stromal cells of the two groups appeared normal under a light microscope (Fig. 1a, b).

We further observed the ultrastructure of the endometrial cells by electron microscopy. Oblong nuclei were found in the stromal cells, and they were surrounded by several normal mitochondria that showed closely packed cristae. There were no significant differences in the ultrastructure of stromal cells between the superovulation group and normal group. However, we did not find uterus gland tissues under the electron microscope, so we were unable to observe the ultrastructure of glandular epithelial cells (Fig. 1c).

*Microscopic and ultramicroscopic structure of the mammary gland*

The normal mammary gland is composed of acini, branching ducts, and connective tissue. The acini are the functional

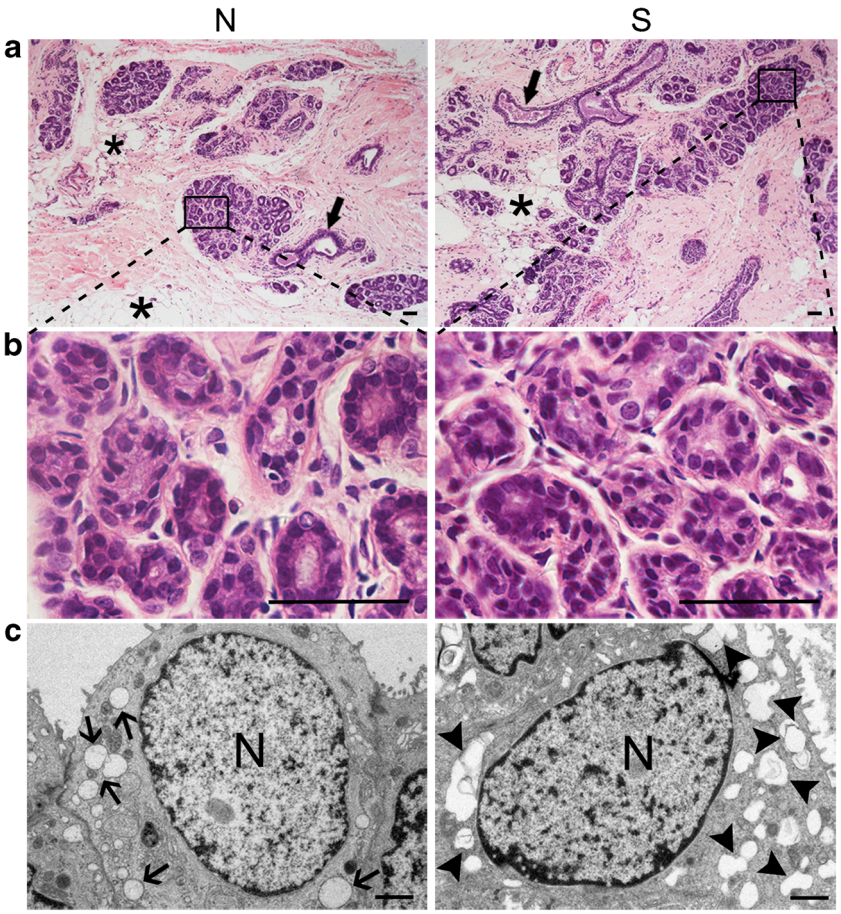


**Fig. 2** Structural analysis of the mammary gland: **a–b** HE staining showed that the mammary gland was normal in histology in both the superovulation group and normal group (duct:➡; fat cells:✱). Scale bar: 50 μm. **c** Irregularly shaped Golgi-derived secretory vesicles were observed in the acini of the superovulation group (normal secretory vesicle:➔; irregularly shaped Golgi-derived secretory vesicles: ➤). Scale bar: 1 μm. *S* = superovulation group; *N* = normal group

secretory units of the mammary gland, which contains glandular epithelial cells and myoepithelial cells. The connective tissues contain many fat cells. In this study, no discernible abnormalities in the cellular morphological or histological characteristics of mammary gland tissue were found in the two groups (Fig. 2a, b).

When we further observed the ultrastructure of glandular epithelial cells under an electron microscope, many irregularly shaped Golgi-derived secretory vesicles were found in the superovulation group. However, the vesicles appeared round and regular in normal mammary gland tissue, as was observed in the normal group (Fig. 2c). The ultrastructural changes in gland epithelial cells may have been a result of repeated stimulation of ovulation.

## Functional assessment of the uterus and mammary gland

### *Proliferation and apoptosis in the uterus*

We assessed uterine function by analyzing the proliferation and apoptosis of cells, which are an indicator of the developmental status of organs. Ki67 and PCNA were used as proliferation markers and detected by immunostaining and Western blot, respectively. As shown in Fig. 3a, Ki67-positive signals were mainly observed in the glandular epithelial cells. We calculated the percentage of Ki67-positive cells and found there was no statistical difference between the normal and superovulation groups ($P > 0.05$; Fig. 3d). However, the relative content of PCNA was significantly lower in the superovulation group than that in the normal group ($P < 0.05$; Fig. 3c, e).

We used the TUNEL assay and a caspase-3 Western blot to evaluate apoptotic status. The TUNEL-positive signals were also observed in the glandular epithelial cells (Fig. 3b). By calculating the percentage of TUNEL-positive cells and the relative content of cleaved caspase-3, we found that there were no significant differences in the apoptotic indices between the normal and superovulation groups ($P > 0.05$; Fig. 3c–e).

### *Proliferation and apoptosis in the mammary gland*

Using Western blot, we detected the expression of PCNA to assess the proliferation status of the mammary gland cells. As shown in Fig. 4b, d, the relative content of PCNA was significantly lower in the superovulation group compared with the normal group ($P < 0.05$).

The TUNEL assay and caspase-3 Western blot were used as indicators for evaluation of apoptotic status. The specific

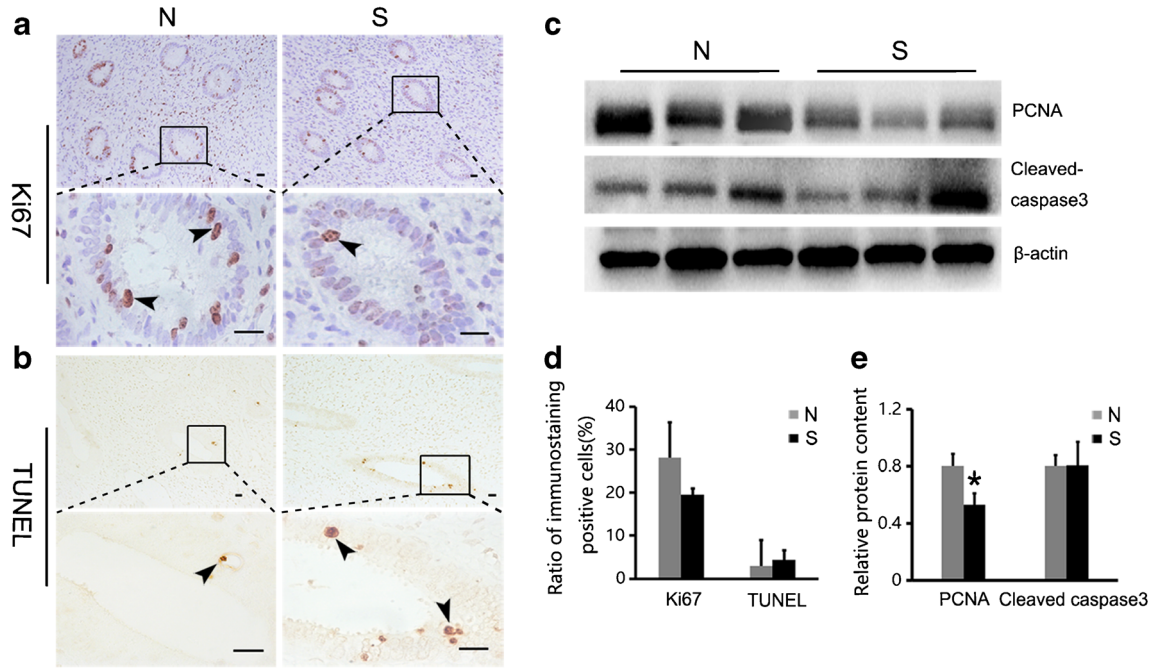


**Fig. 3** Proliferation and apoptosis in the uterus: **a** Uterus of superovulated monkeys was stained with anti-ki67 antibody and compared with stained sections from normal monkey. The positive cells rate of the uterine glandular epithelium were counted (**d**) (positive cells:➤; $P > 0.05$). Scale bar: 20 μm. **b** TUNEL-positive signals were detected mainly in the uterine glandular epithelial cells (positive cells:➤). Ratio of positive cell is shown in (**d**) ($P > 0.05$). Scale bar: 20 μm. **c** and **e** The expression of uterine proliferation and apoptosis markers were analyzed by Western blot: the relative content of PCNA was significantly lower in the superovulation group compared with the normal group ($P < 0.05$), and the relative content of cleaved caspase-3 was not significantly different between the normal and superovulation groups ($P > 0.05$). *Asterisks* mark statistical significance ($P < 0.05$) compared to normal monkeys. *S* = superovulation group; *N* = normal group

TUNEL-positive signal was observed in glandular epithelial cells of both the normal and superovulation groups (Fig. 4a), but the positive cell rate was not significantly different between the two groups ($P > 0.05$; Fig. 4c). However, when we calculated the relative content of cleaved caspase-3, we found a significant increase in this marker in the superovulation groups ($P < 0.05$; Fig. 4b, d).

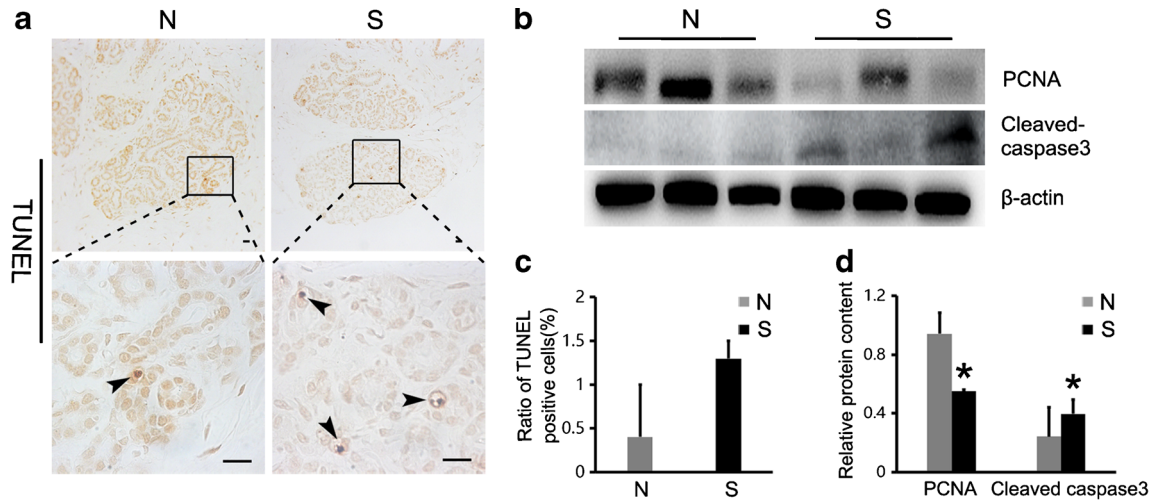


**Fig. 4** Proliferation and apoptosis in the mammary gland: **a** TUNEL-positive cells were observed mainly in the acini (positive cells:➤). The positive cells ratio of TUNEL is shown in (**c**) ($P > 0.05$). Scale bar: 20 μm. **b** and **d** The expression of mammary gland proliferation and apoptosis markers were analyzed by Western blot: the relative content of PCNA and cleaved caspase-3 were significantly different in the superovulation group compared with the normal group ($P < 0.05$). *Asterisks* mark statistical significance ($P < 0.05$) compared with normal monkeys. *S* = superovulation group; *N* = normal group

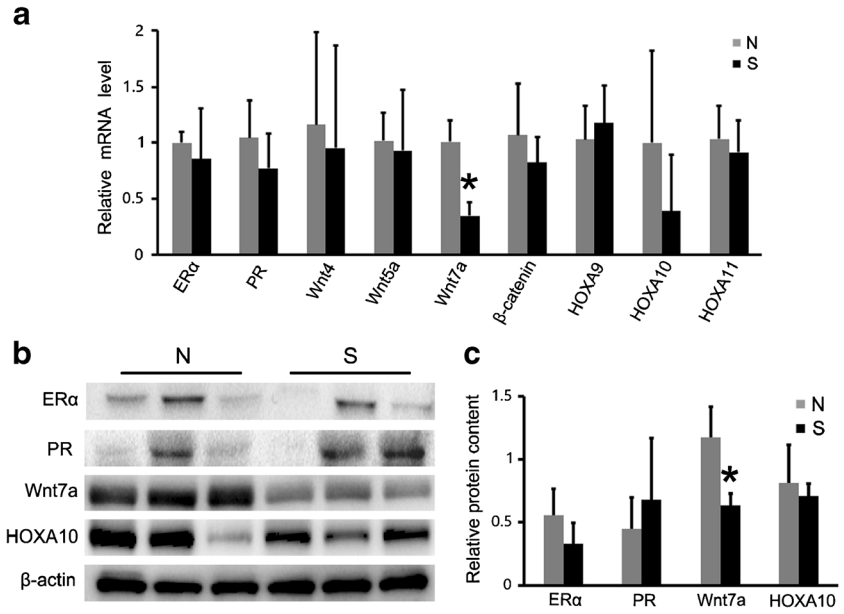


**Fig. 5** Expression of development/function-related genes in the uterus: **a** Changes in the expression of uterine development/function-related genes in the uterine tissues of superovulated monkeys, in comparison with the expression of these genes in normal monkeys. Wnt7a showed significantly lower expression in the superovulation group than in the normal group ($P < 0.05$). **b–c** The lower expression of Wnt7a was further confirmed at the protein level by Western blot ($P < 0.05$). *Asterisks* mark statistical significance ($P < 0.05$) compared with normal monkeys. *S* = superovulation group; *N* = normal group

*Expression of development/function-related genes in the uterus*

To further assess the developmental and functional status of the uterus, we examined the mRNA levels of nine uterus development/function-related genes (ERα, PR, Wnt4, Wnt5a, Wnt7a, β-catenin, HOXA9, HOXA10, and HOXA11). In the uterine tissue, the mRNA level of Wnt7a showed significantly lower expression in the superovulation group than in the normal group ($P < 0.05$; Fig. 5a), and the

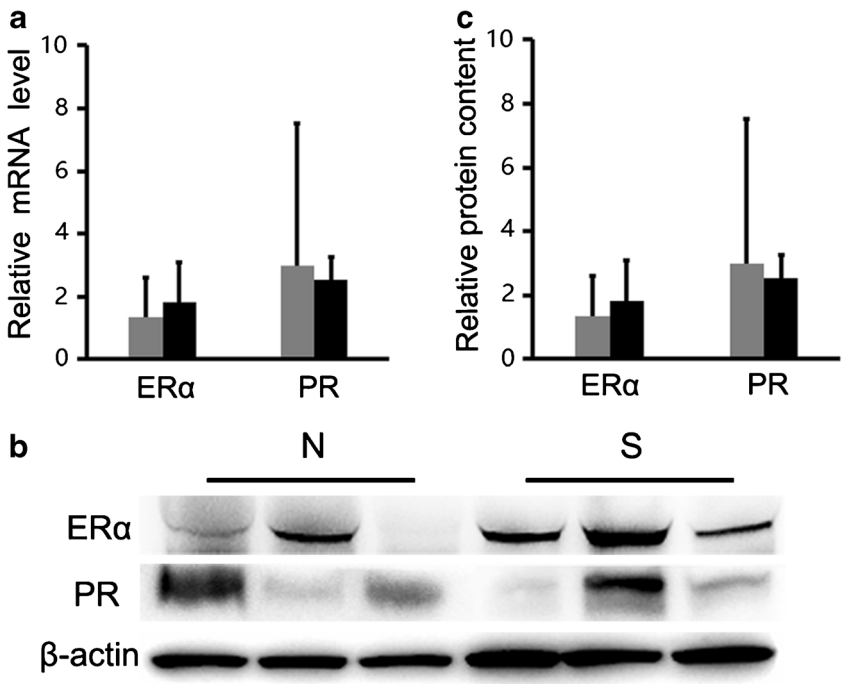


**Fig. 6** Expression of development/function-related genes in the mammary gland: **a** The mRNA levels of ERα and PR were not significantly different between the superovulation and normal groups ($P > 0.05$). **b–c** The protein levels of ERα and PR were consistent with normal group ($P > 0.05$). *S* = superovulation group; *N* = normal group

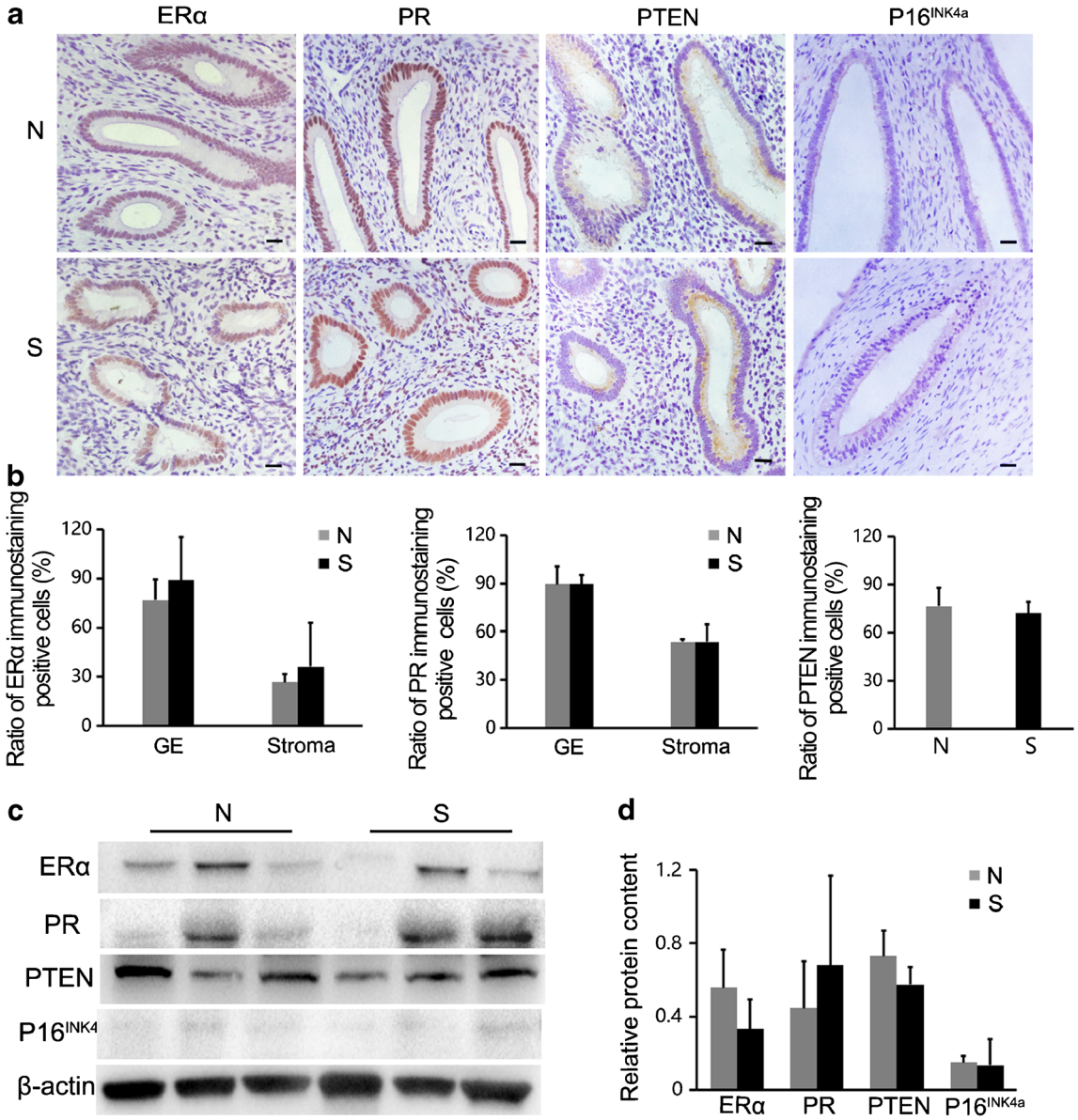


**Fig. 7** Cancer markers in the uterus: **a–b** Immunostaining detection of four uterine tumor molecular markers; the positive cell rates were not significantly different between the two groups ($P > 0.05$). Scale bar: 20 μm. **c–d** The expression of ERα, PR, PTEN and $P16^{INK4a}$ was analyzed by Western blot: their expression was not significantly different between the superovulation and normal groups ($P > 0.05$). *S* = superovulation group; *N* = normal group; *GE* = glandular epithelium

lower expression of Wnt7a was further confirmed at the protein level by Western blot ($P < 0.05$; Fig. 5b, c). The expression of the other eight uterine genes was not significantly different between the two groups ($P > 0.05$; Fig. 5).

*Expression of development/function-related genes in the mammary gland*

In the mammary gland tissue, ERα and PR as the functional markers were detected by real-time PCR and Western blot. The results showed the expression levels of ERα and PR were not significantly different in the normal and superovulation groups, both at the mRNA and protein level ($P > 0.05$; Fig. 6).

## Assessment of cancer markers in the uterus and mammary gland

*Cancer markers in the uterus*

Manual as well as light microscopy examination did not reveal the presence of any lumps in the uterus of monkeys in the superovulation group. Therefore, we analyzed the levels of common tumor molecular markers

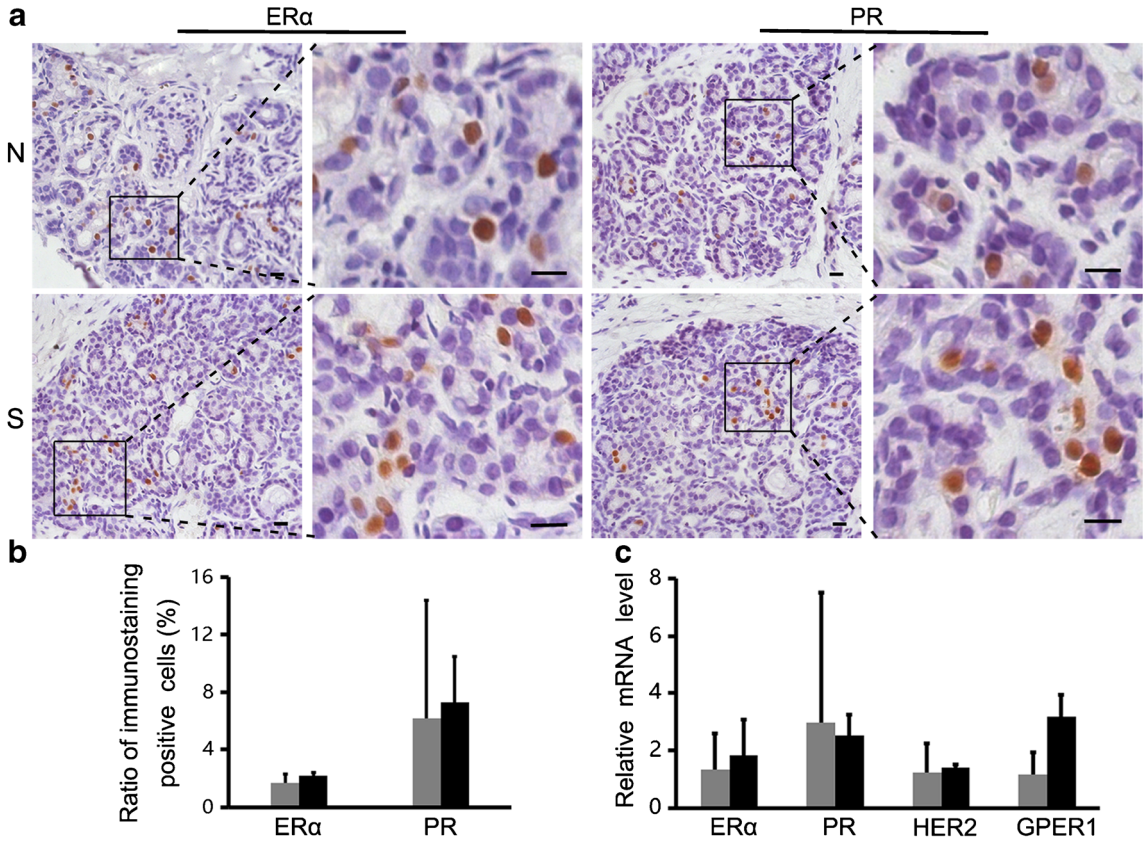


**Fig. 8** Cancer markers in the mammary gland: **a–b** Immunostaining detection of tumor molecular markers (ERα, PR); the positive cell rates not significantly different between the two groups ($P > 0.05$). Scale bar: 20 μm. **c** The expression of four mammary gland tumor molecular markers was analyzed by real-time PCR: their expression was not significantly different between the superovulation and normal groups ($P > 0.05$). *S* = superovulation group; *N* = normal group

to determine whether repeated COH is associated with increased cancer risk. ERα, PR, PTEN, and $P16^{INK4a}$ were selected as the uterine tumor markers for assay. By observing the immunohistochemical results, we found that ERα and PR were expressed diffusely in the glandular epithelium and stromal cells, and PTEN was only expressed in the glandular epithelium. However, no obvious $P16^{INK4a}$-positive signals were found in uterine cells for both groups (Fig. 7a). By calculating the ratio of positive cells, we demonstrated similar expression of these markers in the normal and superovulation groups ($P > 0.05$; Fig. 7b). Moreover, we detected the expression of the four markers by Western blot. The relative contents of the four proteins were not significantly different between the normal and superovulation groups ($P > 0.05$; Fig. 7c, d).

*Cancer markers in the mammary gland*

We also analyzed the expression of several molecular markers of the mammary cancer, including ERα, PR, HER2, and GPER1. The immunochemical staining showed that ERα and PR were mainly expressed in glandular epithelial cells of the normal and superovulation groups (Fig. 8a), but the ratio of positive cells was not significantly different between the two groups ($P > 0.05$; Fig. 8b). Furthermore, the real-time PCR analysis indicated similar expression levels of the four markers in the mammary gland of the normal and superovulated monkeys ($P > 0.05$; Fig. 8c).

## Discussion

In this study, we have assessed the long-term effects of repeated COH by observing the uterus and mammary gland of rhesus monkeys 5 years after they underwent four cycles of ovarian stimulation.

With regard to the effect of repeated COH on the structure of reproductive organs, we found no significant structural abnormalities in the uterus of the COH monkeys. However, we were unable to observe the ultrastructure of the glandular epithelial cells, so we may have missed some ultrastructural changes in the uterus. When we further assessed the developmental/functional status of the uterus, we found a

significant decrease in the proliferation index in the superovulated monkeys, suggesting the low developmental state of uterine cells. Moreover, the decreased expression of the uterus development-related gene was also found in the superovulated monkeys.

The WNT signaling pathway and HOX gene family have been reported to be associated with the development and function of the uterus. Some WNT signaling-related proteins, including Wnt4, Wnt5a, Wnt7a, and β-catenin, have been proven to be critical for uterine development, participating in Müllerian duct initiation, stromal cell decidualization, epithelial–mesenchymal interactions, etc. [23–27]. Thereinto, Wnt7a has been demonstrated to be necessary for the differentiation of the uterine glands [25, 26]. The HOX gene family is linked with uterine development because HOXA9, HOXA10, and HOXA11 are reported to be required for endometrial development and receptivity [28–30]. In this study, we found that the expression level of Wnt7a decreased significantly in the superovulation group, which indicated that repeated ovulation stimulation might affect the development of uterine glands.

In the mammary gland, ultrastructural analysis revealed that the Golgi-derived secretory vesicles were irregular in shape in the superovulation group. It is known that the development and function of the mammary gland is mainly regulated by prolactin (PRL), which can induce acini growth and stimulate lactogenesis [31]. The effect of PRL on lactogenesis relies on a phosphorylation step [32], which takes place in the Golgi apparatus. Thus, the change observed in the structure of the Golgi apparatus of mammary gland cells may have affected the function of PRL in the superovulation group.

The low development status of the mammary gland cells in the superovulated monkeys was further confirmed by the results of molecular marker detection. Although the expression of ERα and PR, two mammary gland development-related genes [33, 34], were not significantly different for the superovulation and normal groups, the significant decrease in the proliferation index as well as the increase in the apoptosis index was demonstrated in the superovulated monkeys.

In addition to investigating the structure and function of the uterus and mammary gland, we also assessed the risk of cancer in these two organs after superovulation. As manual and light microscopy examination did not reveal the presence of any lumps in the uterus or mammary gland of the superovulation group, we analyzed the expression of common tumor markers, including the uterine tumor markers ERα, PR, PTEN, and $P16^{INK4a}$ [35–37] and the mammary gland tumor markers ERα, PR, HER2, and GPER1 [38–40]. Our data showed that the expression of these tumor markers was not different between the normal and superovulation groups. It has been shown that the cancer risk increases with increase in the time that elapses after COH [41]. In our study, the samples were obtained from rhesus monkeys that had undergone stimulated ovulation for 5 years. It is possible that the interval was too short, and there is a possibility of tumor formation after a longer period of time.

In summary, the repeated induction of ovulation was found to affect the expression of the uterine development-related gene Wnt7a several years later, and the uterine cells exhibited a low proliferation status. The ultrastructure of the mammary gland epithelial cells was demonstrated to be abnormal, and the mammary gland cells exhibited a low proliferation and high apoptosis status. Although this study did not find severe damage to the structure of the uterus or mammary gland after repeated COH, the organs exhibited potential low developmental competence. Moreover, we cannot rule out the possibility of damage or more obvious changes in these organs after a longer duration of time. To our knowledge, this is the first time a study, using monkeys as an animal model, has demonstrated an effect of repeated COH on the uterus and mammary gland. Given that the primate is the closest relative of humans, the results obtained from this study provide more intuitive information for optimization of clinical COH. Combined with our previous findings that demonstrated an obvious impact of repeated COH on the ovaries, we propose the need to reconsider the dose of administered gonadotropin and the number of cycles of ovarian hyperstimulation performed.

**Acknowledgments** This work was supported by grants from the National Science Foundation of China (no. 31271604) and the Major State Basic Research Development Program of China (973 Program) (no. 2012CB944902).

## References

1. Ge H, Tollner TL, Hu Z, Da M, Li X, Guan H, et al. Impaired mitochondrial function in murine oocytes is associated with controlled ovarian hyperstimulation and in vitro maturation. Reprod Fertil Dev. 2012;24:945–52.
2. Burwinkel TH, Buster JE, Scoggan JL, Carson SA. Basal follicle stimulating hormone (FSH) predicts response to controlled ovarian hyperstimulation (COH)-intrauterine insemination (IUI) therapy. J Assist Reprod Genet. 1994;11:24–7.
3. Luk J, Arici A. Does the ovarian reserve decrease from repeated ovulation stimulations? Curr Opin Obstet Gynecol. 2010;22:177–82.
4. Diamond MP, DeCherney AH, Hill GA, Nero F, Wentz AC. Response to repetitive cycles of ovulation induction in the same women. J In Vitro Fert Embryo Transf. 1987;4:251–5.
5. Chao HT, Lee SY, Lee HM, Liao TL, Wei YH, Kao SH. Repeated ovarian stimulations induce oxidative damage and mitochondrial DNA mutations in mouse ovaries. Ann N Y Acad Sci. 2005;1042:148–56.
6. Di Luigi G, Rossi G, Castellucci A, Leocata P, Carta G, Canipari R, et al. Repeated ovarian stimulation does not affect the expression level of proteins involved in cell cycle control in mouse ovaries and fallopian tubes. J Assist Reprod Genet. 2014;31:717–24.
7. Kalthur G, Salian SR, Nair R, Mathew J, Adiga SK, Kalthur SG, et al. Distribution pattern of cytoplasmic organelles, spindle integrity, oxidative stress, octamer-binding transcription factor 4 (Oct4)

expression and developmental potential of oocytes following multiple superovulation. Reprod Fertil Dev. 2015;28:2027–2038.
8. Abbott DH, Foong SC, Barnett DK, Dumesic DA. Nonhuman primates contribute unique understanding to anovulatory infertility in women. ILAR J. 2004;45:116–31.
9. Yang S, He X, Hildebrandt TB, Zhou Q, Ji W. Superovulatory response to a low dose single-daily treatment of rhFSH dissolved in polyvinylpyrrolidone in rhesus monkeys. Am J Primatol. 2007;69:1278–84.
10. Yang S, He X, Hildebrandt TB, Jewgenow K, Goeritz F, Tang X, et al. Effects of rhFSH dose on ovarian follicular response, oocyte recovery and embryo development in rhesus monkeys. Theriogenology. 2007;67:1194–201.
11. Dong GY, Guo YS, Cao HR, Zhou T, Zhou ZM, Sha JH, et al. Long-term effects of repeated superovulation on ovarian structure and function in rhesus monkeys. Fertil Steril. 2014;102:1452–7.
12. Althuis MD, Moghissi KS, Westhoff CL, Scoccia B, Lamb EJ, Lubin JH, et al. Uterine cancer after use of clomiphene citrate to induce ovulation. Am J Epidemiol. 2005;161:607–15.
13. Brinton LA, Scoccia B, Moghissi KS, Westhoff CL, Niwa S, Ruggieri D, et al. Long-term relationship of ovulation-stimulating drugs to breast cancer risk. Cancer Epidemiol Biomarkers Prev. 2014;23:584–93.
14. van Leeuwen FE, Klip H, Mooij TM, van de Swaluw AM, Lambalk CB, Kortman M, et al. Risk of borderline and invasive ovarian tumours after ovarian stimulation for in vitro fertilization in a large Dutch cohort. Hum Reprod. 2011;26:3456–65.
15. Sanner K, Conner P, Bergfeldt K, Dickman P, Sundfeldt K, Bergh T, et al. Ovarian epithelial neoplasia after hormonal infertility treatment: long-term follow-up of a historical cohort in Sweden. Fertil Steril. 2009;91:1152–8.
16. Dos Santos S, Wark PA, McCormack VA, Mayer D, Overton C, Little V, et al. Ovulation-stimulation drugs and cancer risks: a long-term follow-up of a British cohort. Br J Cancer. 2009;100:1824–31.
17. Brinton LA, Lamb EJ, Moghissi KS, Scoccia B, Althuis MD, Mabie JE, et al. Ovarian cancer risk after the use of ovulation-stimulating drugs. Obstet Gynecol. 2004;103:1194–203.
18. Dor J, Lerner-Geva L, Rabinovici J, Chetrit A, Levran D, Lunenfeld B, et al. Cancer incidence in a cohort of infertile women who underwent in vitro fertilization. Fertil Steril. 2002;77:324–7.
19. Jensen A, Sharif H, Svare EI, Frederiksen K, Kjaer SK. Risk of breast cancer after exposure to fertility drugs: results from a large Danish cohort study. Cancer Epidemiol Biomarkers Prev. 2007;16:1400–7.
20. Yang S, He X, Niu Y, Wang X, Lu B, Hildebrandt TB, et al. Dynamic changes in ovarian follicles measured by ultrasonography during gonadotropin stimulation in rhesus monkeys. Theriogenology. 2009;72:560–5.
21. Calhoun KC, Padilla-Banks E, Jefferson WN, Liu L, Gerrish KE, Young SL, et al. Bisphenol A exposure alters developmental gene expression in the fetal rhesus macaque uterus. PLoS ONE. 2014;9:e85894.
22. Yu Y, Zhao C, Lv Z, Chen W, Tong M, Guo X, et al. Microinjection manipulation resulted in the increased apoptosis of spermatocytes in testes from intracytoplasmic sperm injection (ICSI) derived mice. PLoS ONE. 2011;6:e22172.
23. Franco HL, Dai D, Lee KY, Rubel CA, Roop D, Boerboom D, et al. WNT4 is a key regulator of normal postnatal uterine development and progesterone signaling during embryo implantation and decidualization in the mouse. FASEB J. 2011;25:1176–87.
24. Mericskay M, Kitajewski J, Sassoon D. Wnt5a is required for proper epithelial-mesenchymal interactions in the uterus. Development. 2004;131:2061–72.
25. Carta L, Sassoon D. Wnt7a is a suppressor of cell death in the female reproductive tract and is required postnatal and estrogen-mediated growth. Biol Reprod. 2004;71:444–54.
26. Parr BA, McMahon AP. Sexually dimorphic development of the mammalian reproductive tract requires Wnt-7a. Nature. 1998;395:701–10.
27. Ingaramo PI, Milesi MM, Schimpf MG, Ramos JG, Vigezzi L, Muñoz-de-Toro M, et al. Endosulfan affects uterine development and functional differentiation by disrupting Wnt7a and β-catenin expression in rats. Mol Cell Endocrinol. 2016;425:37–47.
28. Akbas GE, Taylor HS. HOXC and HOXD gene expression in human endometrium: lack of redundancy with HOXA paralogs. Biol Reprod. 2004;70:39–45.
29. Xu B, Geerts D, Bu Z, Ai J, Jin L, Li Y, et al. Regulation of endometrial receptivity by the highly expressed HOXA9, HOXA11 and HOXD10 HOX-class homeobox genes. Hum Reprod. 2014;29:781–90.
30. Benson GV, Lim H, Paria BC, Satokata I, Dey SK, Maas RL. Mechanisms of reduced fertility in Hoxa-10 mutant mice: uterine homeosis and loss of maternal Hoxa-10 expression. Development. 1996;122:2687–96.
31. Freeman ME, Kanyicska B, Lerant A, Nagy G. Prolactin: structure, function, and regulation of secretion. Physiol Rev. 2000;80:1523–631.
32. Hennighausen L, Robinson GW, Wagner KU, Liu W. Prolactin signaling in mammary gland development. J Biol Chem. 1997;272:7567–9.
33. Aupperlee MD, Haslam SZ. Differential hormonal regulation and function of progesterone receptor isoforms in normal adult mouse mammary gland. Endocrinology. 2007;148:2290–300.
34. Shyamala G, Chou YC, Nandi S, Guzman RC, Smith GH, Nandi S. Cellular expression of estrogen and progesterone receptors in mammary glands: regulation by hormones, development and aging. J Steroid Biochem Mol Biol. 2002;80:137–48.
35. Kreizman-Shefer H, Pricop J, Goldman S, Elmalah I, Shalev E. Distribution of estrogen and progesterone receptors isoforms in endometrial cancer. Diagn Pathol. 2014;9:77.
36. Yoo SH, Park BH, Choi J, Yoo J, Lee SW, Kim YM, et al. Papillary mucinous metaplasia of the endometrium as a possible precursor of endometrial mucinous adenocarcinoma. Mod Pathol. 2012;25:1496–507.
37. Yaginuma Y, Yamashita T, Ishiya T, Morizaki A, Katoh Y, Takahashi T, et al. Abnormal structure and expression of PTEN/MMAC1 gene in human uterine cancers. Mol Carcinog. 2000;27:110–6.
38. Cornejo KM, Kandil D, Khan A, Cosar EF. Theranostic and molecular classification of breast cancer. Arch Pathol Lab Med. 2014;138:44–56.
39. Zhao L, Yang X, Khan A, Kandil D. Diagnostic role of immunohistochemistry in the evaluation of breast pathology specimens. Arch Pathol Lab Med. 2014;138:16–24.
40. Filardo EJ, Graeber CT, Quinn JA, Resnick MB, Giri D, DeLellis RA, et al. Distribution of GPR30, a seven membrane-spanning estrogen receptor, in primary breast cancer and its association with clinicopathologic determinants of tumor progression. Clin Cancer Res. 2006;12:6359–66.
41. Chene G, Penault-Llorca F, Le Bouëdec G, Mishellany F, Dauplat MM, Jaffeux P, et al. Ovarian epithelial dysplasia after ovulation induction: time and dose effects. Hum Reprod. 2009;24:132–8.